Available online at www.sciencedirect.com
SCIENCE DIRECT®

Journal of the European Ceramic Society 24 (2004) 2785–2791
www.elsevier.com/locate/jeurceramsoc

Reaction sintered Al_2O_3/Al_2TiO_5 microcrack-free composites obtained by colloidal filtration

S. Bueno, R. Moreno, C. Baudín*

Instituto de Cerámica y Vidrio, C.S.I.C- Campus de Cantoblanco, Camino de Valdelatas s/n, 28049 Madrid, Spain

Received 8 June 2003; received in revised form 22 August 2003; accepted 30 August 2003

Abstract

Dense and microcrack-free Al_2O_3/Al_2TiO_5 composites (10, 30 and 40 vol.% of Al_2TiO_5) have been obtained by colloidal filtration and reaction sintering, using alumina and titania as starting powders. The processing of the composites has been studied focusing on the rheological behaviour of aqueous suspensions of each powder and of mixtures. Colloidal filtration of optimised suspensions, with a solid loading as high as 50 vol.%, and a thermal treatment at 1450 °C, lead to completely reacted and uncracked sintered materials with homogeneously distributed aluminium titanate contents up to 40 vol.% and high density. Thermal diffusivity values from 25 to 800 °C are coincident on heating and cooling for the three studied composites, and decrease with temperature and with aluminium titanate content.

Keywords: Al_2O_3; Al_2TiO_5; Composites; Slip casting; Thermal conductivity

1. Introduction

Alumina (Al_2O_3)–aluminium titanate (Al_2TiO_5) composites can offer improved flaw tolerance and toughness.[1–6] Aluminium titanate is highly anisotropic ($\alpha_{a25-1000^\circ C} = 10.9 \cdot 10^{-6}\ ^\circ C^{-1}$, $\alpha_{b25-1000^\circ C} = 20.5 \times 10^{-6}\ ^\circ C^{-1}$, $\alpha_{c25-1000^\circ C} = -2.7 \times 10^{-6}\ ^\circ C^{-1}$),[7] therefore, even though the average crystallographic thermal expansion of aluminium titanate is slightly higher than that of alumina ($\alpha_{A25-1000^\circ C} = 8.7 \times 10^{-6}\ ^\circ C^{-1}$, $\alpha_{AT25-1000^\circ C} = 9.7 \times 10^{-6}\ ^\circ C^{-1}$),[7,8] high compressive residual stresses on the aluminium titanate grains are expected to develop during cooling from the sintering temperature, at least for some grain-matrix crystallographic orientations. Consequently, Al_2TiO_5 grains may act as bridges during fracture. Moreover microcracking may also occur during fracture due to the residual stresses.

The characteristics of the toughness curve and, therefore, the flaw tolerance of alumina–aluminium titanate composites may be strongly modified by appropriately altering the microstructure. There is a range of volume fraction–particle size in which stable microcrack growth occurs during loading, leading to nonlinear stress–strain behaviour and to an enlargement of the range of crack sizes for which the material is flaw tolerant. Limits are imposed by the possible coalescence of multiple microcracks and, consequently, loss of strength.[6,9]

Moreover, due to the extreme local stresses that develop in alumina–aluminium titanate composites, spontaneous microcracking usually occurs during cooling from the sintering temperature and coalescence of these microcracks may even nucleate the failure of the unloaded material. In this sense, the microstructure of the materials has to be controlled to reach sufficient stress level to obtain the desired non-linear stress–strain behaviour without generalised failure. In this sense, increasing contents of aluminium titanate particles of controlled size would improve the mechanical response of the composites.

Dense alumina–aluminium titanate composites with controlled microstructure have been fabricated from alumina and previously reacted aluminium titanate powders.[1,2,5,6,10] Another way to fabricate such composites which, in principle, appears as more attractive in terms of energy saving, is by the reaction sintering of alumina and titania (TiO_2) mixtures,[3,4,11] Most resultant

* Corresponding author. Tel.: +34-91-871-1800; fax: +34-91-870-0550.
E-mail address: cbaudin@icv.csic.es (C. Baudín).

0955-2219/$ - see front matter © 2003 Elsevier Ltd. All rights reserved.
doi:10.1016/j.jeurceramsoc.2003.08.015

microstructures obtained by reaction sintering display low as-fired densities, abnormal grain growth and even unreacted titania particles, due to the special characteristics of the alumina–titania reaction process.[12–14] A previous work[11] reported that a careful control of processing green compacts made of alumina powders covered by a titania precursor allowed the attainment of high density (~98% of theoretical) in alumina with up to 20 vol.% of aluminium titanate materials. However, composites with larger second phase contents (~20 – 40 vol.%) gave lower densities (~95% of theoretical).

In this work, the possibility of obtaining completely reacted and dense alumina–aluminium titanate composites with controlled microstructure by reaction sintering of alumina and titania powders prepared by colloidal processing is investigated.

In order to achieve homogeneous microstructures with uniform distribution of the second phase and completely reacted aluminium titanate, a strict control of the colloidal properties of the mixture and the thermal treatment has to be accomplished. The colloidal behaviour of titania in water has been extensively studied,[15] as well as the stability of moderately concentrated suspensions.[16] However, concentrated TiO_2 suspensions in water exhibit a marked adhesive character and stick to tools and containers, thus impeding homogeneous mixing. As a consequence, concentrated TiO_2 suspensions display a strong dilatancy, which might be responsible for heterogeneity of the $Al_2O_3 + TiO_2$ compacts obtained previously with colloidal dispersion methods.[16] In this work, the dispersing conditions were optimised through rheological characterisation to obtain suspensions with high solids content (i.e. 50 vol.%) and low viscosity.

The sintering schedule was adjusted in order to achieve complete reaction and densification of the compacts avoiding extensive grain growth.

Many properties of microcracked materials present strong hysteresis while heating and cooling due to crack closure and healing at high temperatures and re-microcracking during cooling. In particular, a significant hysteresis effect on thermal diffusivity was reported for $MgTi_2O_5$ and Fe_2TiO_5 polycrystalline ceramics.[17,18] Hence, microstructural observations and the evolution of thermal diffusivity with temperature have been used to analyse the influence of the volume fraction of aluminium titanate on microcrack formation.

1.1. Experimental

Alumina based composites with 10, 30 and 40 vol.% of Al_2TiO_5, (A10AT, A30AT, and A40AT) were obtained by reaction sintering of green compacts prepared from mixtures of Al_2O_3 and TiO_2 with relative TiO_2 contents of 5, 15 and 20 wt.%. High purity commercial powders of α-Al_2O_3 (Condea, HPA05 without MgO, USA, $d_{50} = 0.35$ μm, specific surface area: 9.5 m^2/g) and TiO_2 (Anatase, Merck, 808, Germany, $d_{50} = 0.35$ μm, specific surface area: 9 m^2/g) were used.

Colloidal stability was determined through zeta potential measurements by microelectrophoresis (Zeta-Meter, 3.0+, USA) for TiO_2 and Al_2O_3 suspensions prepared to a solid loading of 0.01 wt.%; pH was adjusted by addition of either HCl or tetramethylammonium hydroxide (TMAH), and 10^{-2} M KCl was used as inert electrolyte to control the ionic strength. A carbonic acid based polyelectrolyte (Dolapix CE64, Zschimmer-Schwarz, Germany) was used as the dispersing aid. The influence of the polyelectrolyte concentration on the zeta potential was also investigated.

Aqueous suspensions of each powder and their mixtures were prepared to a solid loading of 50 vol.% (80 wt.%) by ball milling, using alumina jar and balls. Dispersing conditions were optimised through rheological characterisation of TiO_2 suspensions as a function of dispersant concentration (0.1–1.0 wt.% on a dry solids basis) after 2 h ball milling; later, the effect of milling time was studied to determine the optimum dispersant proportion. Measurements of viscosity were performed with a rotational rheometer (Haake RS50, Germany). Flow curves of the suspensions were determined for a range of shear rates between 0 and 1000 s^{-1} at a constant temperature of 25 °C. Measurements were also performed by operating under controlled stress conditions in order to determine the yield point from the log/log plot of shear stress versus deformation.[19]

The green compacts blocks, 70 × 70 × 12.5 mm^3, were obtained by colloidal filtration on plaster of Paris moulds and dried in air. To obtain the materials the dried blocks were sintered in air in an electrical box furnace (Termiber, Spain) at heating and cooling rates of 2 °C min^{-1} and 2 h dwell at the maximum temperature, 1450 °C.

The densities of the green and sintered compacts were determined by the Archimedes method, using mercury and water, respectively. Theoretical densities were calculated taking values of 3.99 g cm^{-3} for alumina,[20] 3.89 g cm^{-3} for TiO_2 (anatase),[21] 4.25 g cm^{-3} for TiO_2 (rutile)[22] and 3.70 g cm^{-3} for aluminum titanate.[23] The phases present were determined by X - ray diffraction after grinding (Siemens AG, D5000, Germany) and results were processed using the ASTM Files.[20–23]

Microstructural characterisation was performed by scanning electron microscopy (SEM, Zeiss DSM 950, Germany) on polished and thermally etched (1440 °C—1 min) surfaces.

From the sintered blocks, thin discs (diameter = 12.7 mm, thickness = 1 mm) were machined and covered with graphite for thermal diffusivity measurements, which were carried out from room temperature up to 800 °C, on heating and cooling, using the laser flash method (Holometrix ThermalFlash, USA).

2. Results

In Fig. 1 the zeta potential curves as a function of pH are shown for aqueous suspensions of Al_2O_3 and TiO_2, the isoelectric point occurring at pH values of about 9 and 4, respectively. Kosmulski[15] has made an extensive review of the points of zero charge of TiO_2, which range from 2 to 8.9, and the average value is 5.6. Lower values of the ZPC are attributed to the presence of residual phosphate or other anionic impurities in commercial Titania. High absolute values of the zeta potential (> 20 mV) are only reached at very low or very high pH conditions (pH <3 or pH > 12)

Fig. 2 shows the variation of zeta potential as a function of the concentration of dispersant. The best values are found for additive contents of 0.5 and 0.8 wt.% for Al_2O_3 and TiO_2 suspensions, respectively.

The rheological behaviour of concentrated TiO_2 suspensions was initially studied as a function of the deflocculant content. The measured flow curves are shown in Fig. 3, where the lowest viscosity is found for a polyelectrolyte concentration of 0.5 wt.%.

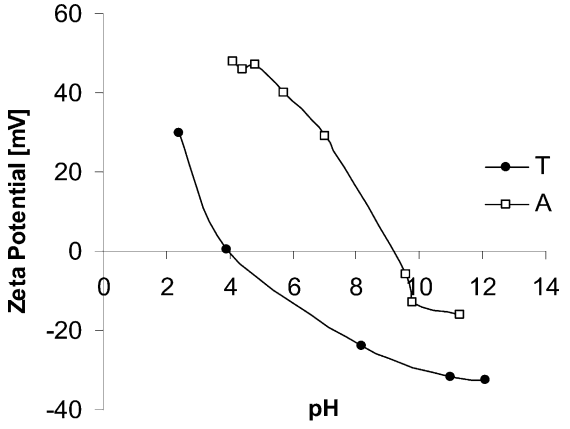

Fig. 1. Zeta potential of alumina (A) and titania (T) as a function of pH.

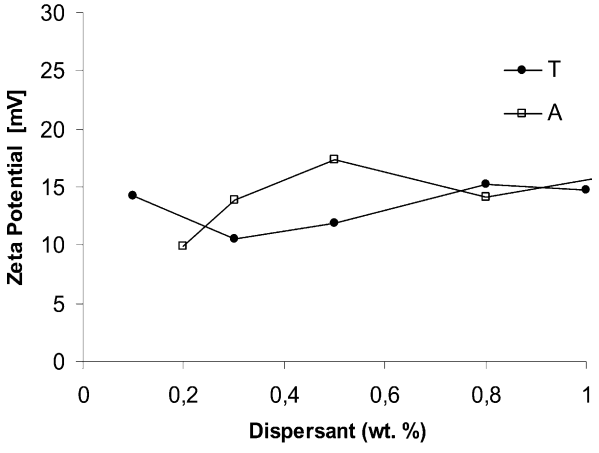

Fig. 2. Zeta potential of alumina (A) and titania (T) with different deflocculant contents.

The effect of milling time on TiO_2 suspensions dispersed with 0.5 wt.% of polyelectrolyte is observed in the flow curves plotted in Fig. 4. For given shear rates, the shear stress diminishes with milling time, but incipient thixotropic behaviour is observed for 6 h and this effect increased for longer milling times. For suspensions ball milled for 1 h and 24 h, the torque of the rheometer was exceeded as a consequence of the strong stickiness of the suspensions, indicating an obvious lack of homogeneity.

Fig. 5 plots the flow curves of Al_2O_3 and TiO_2 slurries as well as their mixtures. Suspensions with 5 and 15 wt.% of TiO_2 are coincident (22 Pa at 500 s^{-1}). A strong difference between Al_2O_3 and TiO_2 aqueous suspensions is observed and the rheological behaviour of the mixture is governed by the major phase. Therefore, deleterious thixotropic effects of TiO_2 suspensions are avoided.

The relative densities of green and sintered samples are summarised in Table 1. The green density of samples obtained by slip casting from the optimised suspensions

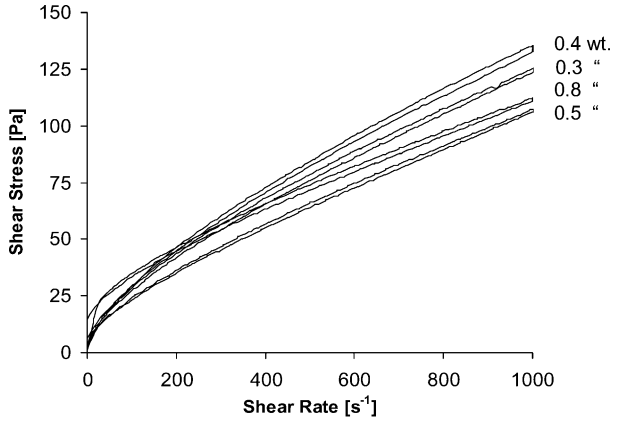

Fig. 3. Flow curve of TiO_2 suspensions with different deflocculant contents after 2 h ball milling.

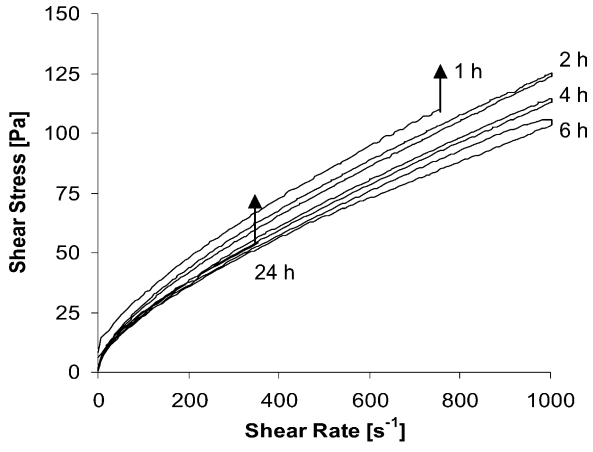

Fig. 4. Flow curve of TiO_2 suspensions after different milling times with 0.5 wt.% of deflocculant content.

Table 1
Relative density of green samples and specimens sintered at 1450 °C

	A	A10AT	A30AT	A40AT	T
Green	64.1±0.5	63.9±0.3	63.4±0.5	62.5±0.2	59.2±0.1
1450 °C–2 h	98.2±0.1	97.4±0.3	97.7±0.5	96.5±0.4	–

Table 2
Viscosity at 500 s^{-1} and yield stress of Al_2O_3–TiO_2 slips with 0.5 wt.% of deflocculant after 4 h milling (A: alumina; T: titania)

	Viscosity (mPa s)	Yield stress (Pa)
A	34	–
A + 5 wt.% T	43	0.16
A + 15 wt.% T	44	0.25
A + 20 wt.% T	51	0.26
T	142	1.18

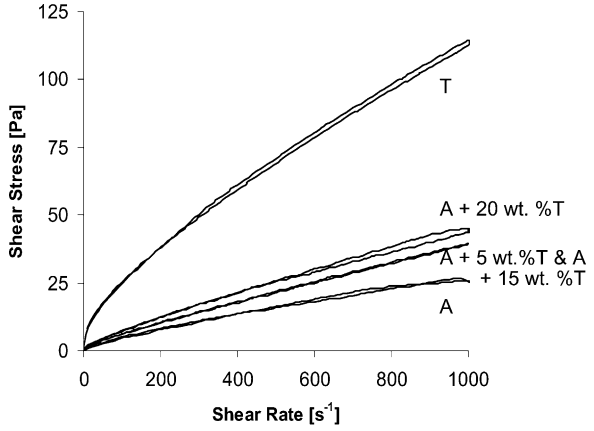

Fig. 5. Flow curve of Al_2O_3–TiO_2 aqueous suspensions after 4 h milling with 0.5 wt.% of deflocculant (A: alumina; T: titania).

tends to slightly decrease for increasing TiO_2 content, although high values, above 62.5% of theoretical, are found in all cases. Sintered density diminishes with aluminium titanate content from ≈97.5 to ≈96.5% of theoretical for the A40AT samples.

The X-ray diffraction profiles in Fig. 6 show the position of characteristic peaks for alumina and aluminium titanate, selected to study the presence of these phases in the three composites. In all cases, the rutile phase was not detected.

Microstructures of the sintered materials are shown in Fig. 7. Only alumina and aluminium titanate were observed by this method (SEM). In all samples, aluminium titanate is homogeneously distributed and located mainly at alumina triple points and grain boundaries. No intragranular porosity is observed in the alumina grains even in the samples with 10vol.% of aluminium titanate (Fig. 7a and b) in which the grain size of alumina (5 μm) is much larger than in the samples containing increased amounts of aluminium titanate

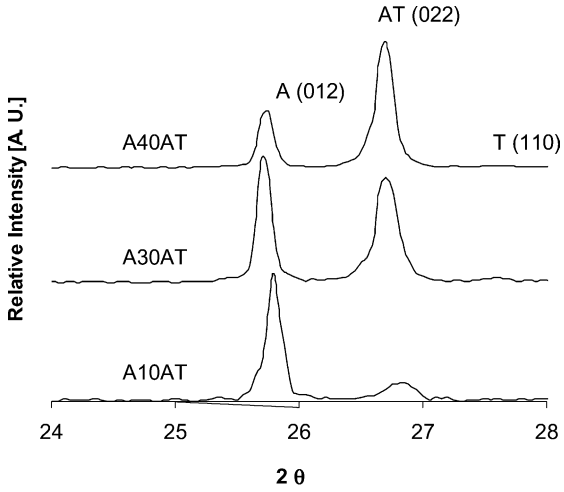

Fig. 6. XRD patterns of composites sintered at 1450 °C–2 h with different aluminium titanate contents (A: α-Al_2O_3; AT: β-Al_2TiO_5; T: TiO_2-rutile).

(Fig. 7c–f). No microcracks are observed in any of the samples.

In Fig. 8 the thermal diffusivity, determined on heating and cooling cycles of the alumina and the three composite materials, is plotted as a function of temperature. For the four studied materials, values on heating and cooling are coincident and decrease with temperature and with aluminium titanate content.

3. Discussion

From zeta potential versus pH curves (Fig. 1), heterogeneous mixtures would be obtained at pH values ranging from 3 to 10, since the particle surfaces of the two powders are oppositely charged, thus leading to heterocoagulation. Hence, purely electrostatic stabilisation is only possible at very aggressive pH conditions. Consequently, the use of a polyelectrolyte capable of providing an electrostatic stabilising mechanism was chosen in order to achieve a good dispersion of the mixtures.

From Fig. 2, well-dispersed mixtures of Al_2O_3 and TiO_2 will be obtained for polyelectrolyte contents larger than 0.5 wt.%. Since Al_2O_3 is the major component of all the compositions studied, a content of 0.5 wt.% of dispersant, coincident with the maximum zeta potential of Al_2O_3, was selected.

The flow curves of TiO_2 slips, ball-milled for 2 h, show a lower viscosity for a dispersant content of 0.5 wt.%, in good agreement with the zeta potential measurements. A higher dispersant content makes for an increased viscosity and leads to Bingham plastic behaviour.

From Fig. 4 the critical influence of milling time on viscosity is obvious. The concentrated TiO_2 slips have a marked sticky character that restricts the effective milling time to a narrow range of times from 2 to 6 h.

However, for 6 h milling some thixotropy develops thus impeding stability over time. In addition, the preparation of the TiO_2/water mixture previous to ball milling was also critical. The powder added to water was first mechanically stirred at different rates. Below 800 rpm the powder stuck to the propeller leading to agglomeration. Above 1000 rpm the suspension became strongly dilatant and no effective mixing was reached.

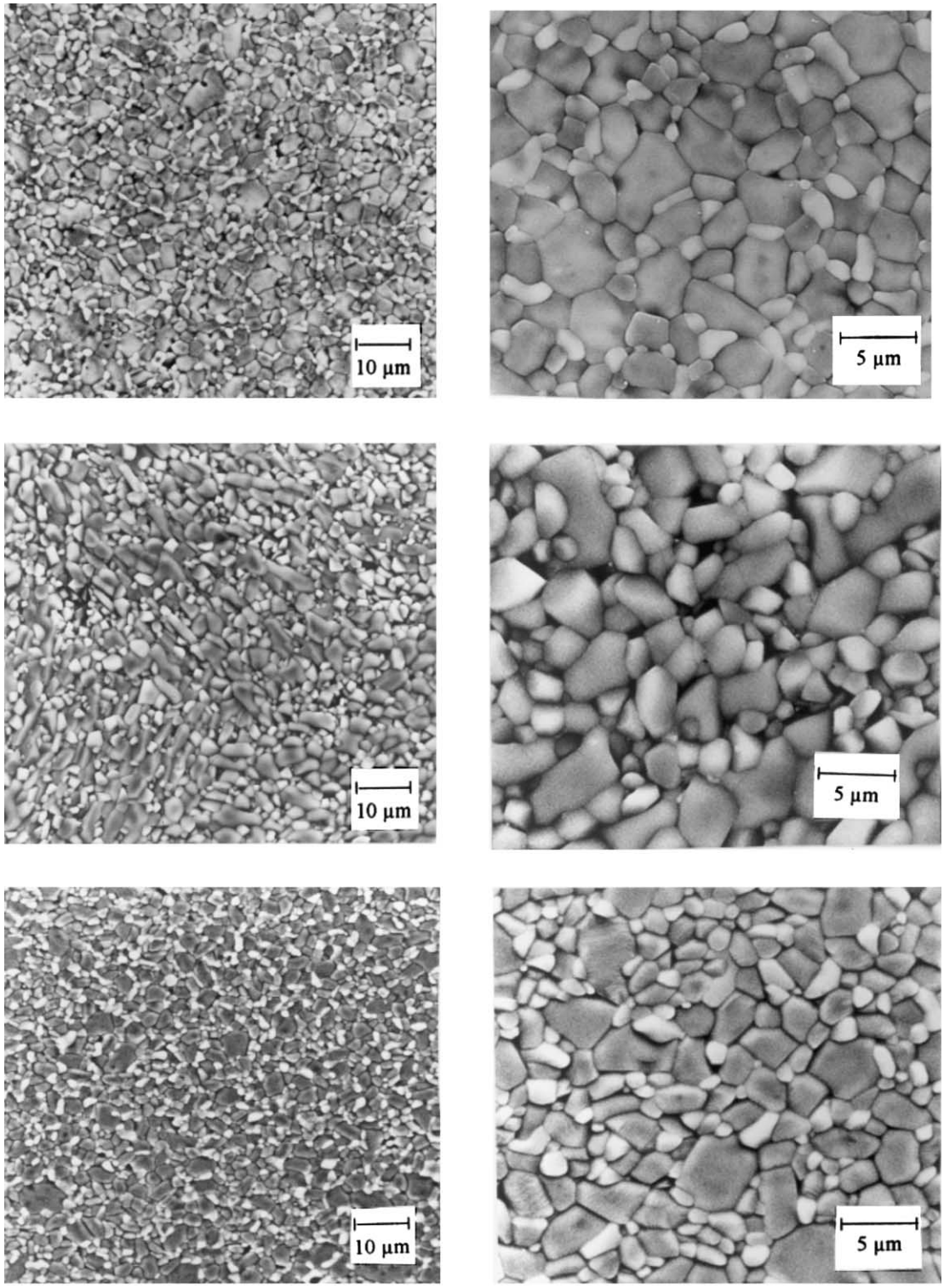

Fig. 7. Scanning electron micrographs of polished and thermally etched (1440 °C–1 min) surfaces of the studied materials A10AT (a, b), A30AT (c, d) and A40AT (e, f). Al_2O_3 grains appear with dark grey colour, Al_2TiO_5 of an intermediate grey shade, whereas TiO_2 would appear white and is not observed.

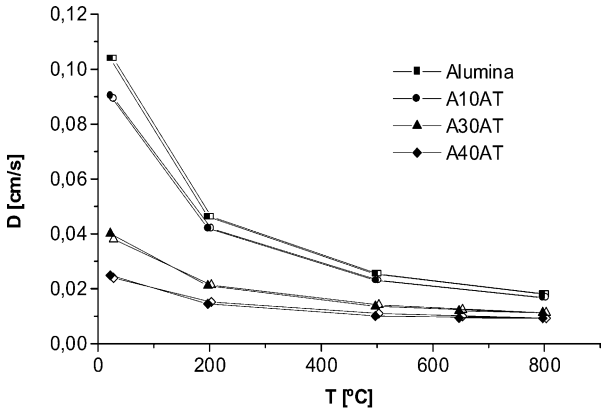

Fig. 8. Diffusivity values during heating and cooling for different aluminium titanate contents (open symbols mean cooling).

Homogeneous slurries could only be prepared by repeated additions of small amounts of TiO_2 powder into the water containing the dispersant stirred at 900 rpm.

The large differences between Al_2O_3 and TiO_2 aqueous suspensions, with the same solids loading, are evident in Fig. 5. The viscosity of the mixtures is controlled by the major phase (Al_2O_3) although the addition of TiO_2 increases the viscosity and incipient thixotropic behaviour arises for the highest TiO_2 content. However, the viscosity remains low enough to allow the slip to be cast easily. Viscosity values of 43, 44 and 51 mPa s were obtained at a shear rate of 500 s^{-1} for mixtures with 5, 15 and 20 wt.% of TiO_2 respectively. Measurements performed under CS (control stress) conditions confirmed the evolution toward plasticity of the mixtures with higher titania contents, with a yield point of more than 1 Pa for the TiO_2 suspension (Table 2). These values are very low considering the high solid loadings (50 vol.%) of the suspensions. The optimised dispersing conditions (4 h ball milling and 0.5 wt.% of dispersant) led to high green density bodies, a consequence of the good stability and homogeneity of the mixtures (Table 1).

The optimised green processing conditions and the thermal treatment at a rather low temperature (1450 °C) led to completely reacted and homogeneous sintered materials (Figs. 6 and 7) with no generalised cracking or microcracks at the SEM scale.

The thermal diffusivity of uncracked aluminium titanate materials is not known due to the difficulties associated with the preparation of dense and uncracked aluminium titanate bodies. Nevertheless, values should be in the range of those of other pseudobrookites, such as $MgTi_2O_5$ or Fe_2TiO_5, (0.009–0.010 cm^2/s)[17,18] which are about one order of magnitude lower than that of alumina (0.100 cm^2/s, Fig. 8). As a consequence, the thermal diffusivity values decrease with aluminium titanate content (Fig. 8).

The temperature dependence of the thermal diffusivity of all materials on heating is typical of uncracked dielectric materials, in which diffusivity decreases with temperature, the opposite to materials in which crack healing at high temperatures (>500 °C) leads to an increase of diffusivity.[17,18] This behaviour agrees with the absence of cracking observed by SEM (Fig. 7) in the composites. Moreover, no differences are found between heating and cooling values for any of the four materials. This fact demonstrates that no, or very little, cracking phenomena occurs in these materials thorough the whole thermal cycle.[17]

4. Conclusions

In this work, the processing parameters to obtain reaction sintered Al_2O_3–Al_2TiO_5 composites from aqueous alumina and titania mixtures have been established.

Well-dispersed mixtures of Al_2O_3 and TiO_2 can be obtained by adding a polyelectrolyte, in amounts greater than 0.5 wt.%. Mixtures with a solids loading of 50 vol.% and without dilatancy can be prepared by strictly controlling the mixing energy and the milling time to get the viscosity of the mixtures controlled by the major phase (Al_2O_3).

Colloidal filtration of optimised suspensions and a thermal treatment at 1450 °C, lead to completely reacted, dense (96.5–98% of theoretical density) and uncracked sintered materials with homogeneously distributed aluminium titanate contents up to 40 vol.%.

Thermal diffusivity values at temperatures from 25 to 800 °C are coincident on heating and cooling, decrease with aluminium titanate content and the temperature dependence is typical of uncracked dielectric materials.

Acknowledgements

This work was supported by the project CICYT MAT 2000-0949 and by the grant CSIC I3P-BPD2001-1 (Spain).

References

1. Runyan, J. L. and Bennison, S. J., Fabrication of flaw-tolerant aluminum–titanate-reinforced alumina. *J. Eur. Ceram. Soc.*, 1991, **7**, 93–99.
2. Padture, N. P., Bennison, S. J. and Chan, H. M., Flaw-tolerance and crack-resistance properties of alumina–aluminium titanate composites with tailored microstructures. *J. Am. Ceram. Soc.*, 1993, **76**, 2312–2320.
3. Bartolomé, J., Requena, J., Moya, J. S., Li, M. and Guiu, F., Cyclic fatigue crack growth resistance of Al_2O_3–Al_2TiO_5 composites. *Acta Mater.*, 1996, **44**, 1361–1370.
4. Bartolomé, J., Requena, J., Moya, J. S., Li, M. and Guiu, F., Cyclic fatigue of Al_2O_3–Al_2TiO_5 composites in direct push–pull. *Fatigue Fract. Engng. Mater. Struct*, 1997, **20**, 789–798.

5. Uribe, R. and Baudín, C., Influence of a dispersion of aluminum titanate particles of controlled size on the thermal shock resistance of alumina. *J. Am. Ceram. Soc.*, 2003, **86**, 846–850.
6. Padture, N. P., Runyan, J. L., Bennison, S. J., Braun, L. M. and Lawn, B. R., Model for toughness curves in two-phase ceramics: II, microstructural variables. *J. Am. Ceram. Soc.*, 1993, **76**, 2241–2247.
7. Taylor, D., Thermal expansion data. XI. Complex oxides, A_2BO_5, and the garnets. *Brit. Cer. Trans. J.*, 1987, **86**, 1–6.
8. Taylor, D., Thermal expansion data: III. Sesquioxides, M_2O_3 with the corundum and the A-, B- and C-M_2O_3. *Brit. Ceram. Trans. J.*, 1984, **83**, 92–98.
9. Lawn, B. R., Padture, N. P., Braun, L. M. and Bennison, S. J., Model for toughness curves in two-phase ceramics: I, basic fracture mechanics. *J. Am. Ceram. Soc.*, 1993, **76**, 2235–2240.
10. Ananthakumar, S. and Warrier, K. G. K., Extrusion characteristics of alumina–aluminium titanate composite using boehmite as a reactive binder. *J. Eur. Ceram. Soc.*, 2001, **21**, 71–78.
11. Okamura, H., Barringer, E. A. and Bowen, H. K., Preparation and sintering of narrow-sized Al_2O_3–TiO_2 composite powders. *J. Mater. Sci.*, 1989, **24**, 1867–1880.
12. Thomas, H. A. J. and Stevens, R., Microstructure development during the reaction sintering of alumina and titania to produce aluminium titanate. In *Br. Ceram. Proc. N° 42.*, ed. R. Stevens and D. Taylor. Stoke-on Trent, UK, 1989, pp. 117–122.
13. Freudenberg, B. and Mocellin, A., Aluminium titanate formation by solid-state reaction of fine Al_2O_3 and TiO_2 powders. *J. Am. Ceram. Soc.*, 1987, **70**, 33–38.
14. Uribe, R. and Baudín, C., Formación de titanato de aluminio por reacción en estado sólido de alúmina y titania. *Bol. Soc. Esp. Ceram. Vidr.*, 2000, **39**, 1–10.
15. Kosmulski, M., The significance of the difference in the point of zero charge between rutile and anatase. *Adv. Colloid Interface Sci.*, 2002, **99**, 255–264.
16. Requena, J., Moya, J. S. and Pena, P., Al_2TiO_5–Al_2O_3 functionally gradient materials obtained by sequential slip casting. *Ceram. Trans*, 1992, **34**, 203–210.
17. Siebeneck, H. J., Hasselman, D. P. H., Cleveland, J. J. and Bradt, R. C., Effect of grain size and microcracking on the thermal diffusivity of $MgTi_2O_5$. *J. Am. Ceram. Soc.*, 1977, **60**, 336–338.
18. Siebeneck, H. J., Hasselman, D. P. H., Cleveland, J. J. and Bradt, R. C., Effect of microcracking on the thermal diffusivity of Fe_2TiO_5. *J. Am. Ceram. Soc.*, 1976, **59**, 241–244.
19. Gutiérrez, C., Sánchez-Herencia, A. J. and Moreno, R., ¿Plástico o pseudoplástico? Métodos de determinación y análisis del punto de fluidez de suspensiones cerámicas. *Bol. Soc. Esp. Ceram. Vidr.*, 2000, **39**, 105–117.
20. *ASTM File 42-1468*. Database PDF (Power Diffraction File).
21. *ASTM File 21-1272*. Database PDF (Power Diffraction File).
22. *ASTM File 21-1276*. Database PDF (Power Diffraction File).
23. *ASTM File 26-0040*. Database PDF (Power Diffraction File).